

# ANALYSIS OF FLUCTUATING PRESSURE AROUND B/D=4 RECTANGULAR SECTION USING PROPER ORTHOGONAL DECOMPOSITION

|         |     |       |         |      |       |
|---------|-----|-------|---------|------|-------|
| 京都大学大学院 | 学生員 | ○李 再炯 | 京都大学大学院 | フェロー | 松本 勝  |
| 京都大学大学院 | 正会員 | 白土博通  | 京都大学大学院 | 正会員  | 八木知己  |
| 阪急電鉄（株） |     | 坪田 樹  | 京都大学大学院 | 学生員  | 堀 高太郎 |

## 1. INTRODUCTION

The aerodynamic excitation of a bluff body immersed in wind is the result of a fluctuating pressure distribution on the body surface which is caused by the shear-layer separated from the leading edge and the vortices generated around the body. Knowledge of the description of the fluctuating pressure allows interpreting the mechanisms of aerodynamic instabilities, and then it can lead to their subsequent suppression and control. In this paper dynamic wind tunnel tests were carried out on the rectangular section with the side ratio 4. Dynamic response and unsteady pressure on the upper surface of the body were measured in the tests. Also Proper Orthogonal Decomposition (POD) was applied to the analysis of the unsteady fluctuating pressure around B/D=4 rectangular section.

## 2. POD ANALYSIS

The Proper Orthogonal Decomposition (POD) is a powerful and effective method for specifying the fluctuating pressure field around structures in recent years. POD is a method of detecting a new coordinate system which can most efficiently represent the original fluctuating phenomena. This method can identify the deterministic or systematic structure hidden in the random fluctuations and thus help us to understand the phenomena better. In this paper, the POD is applied to the unsteady pressure distribution  $P(x, t)$  on the upper surface of the body which can be written as

$$P(x, t) = \sum_{i=1}^n a_i(t) \Phi_i(x)$$

where  $n$  is the number of pressure taps,  $\Phi(x)$  is a normalized proper function and  $a(t)$  is its associated principal component. The proper function  $\Phi(x)$  is the eigenvector of the covariance matrix  $R_p$  of the unsteady pressure distribution.

$$\sum_{i=1}^n R_p(x_j, x_i) W(x_i) \Phi(x_i) = \lambda \Phi(x_j)$$

where  $j=1, 2, \dots, n$ , and  $W(x_i)$  is a weighting function depending on the integration quadrature. For a case of non-uniformly distributed pressure tabs, a modified covariance matrix is introduced, and the modified covariance matrix  $R_p^m(x_i, x_j)$  is non-symmetric. To ensure real eigenvalues and orthogonal eigenvectors in the solution of a discrete eigenvalue problem, it is necessary to keep the matrix Hermitian. To make the covariance matrix symmetric, Eq.(2) is pre-multiplied by

$$W(x_j)^{1/2} \cdot \sum_{i=1}^n R_p^t(x_j, x_i) \Phi^t(x_i) = \lambda \Phi^t(x_j) \quad \text{where } R_p^t(x_j, x_i) = W(x_j)^{1/2} R_p(x_j, x_i) W(x_i)^{1/2} \text{ and } \Phi^t(x_j) = W(x_j)^{1/2} \Phi(x_j), (i, j)$$

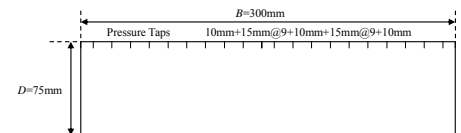


Fig.1 B/D=4 rectangular cylinder

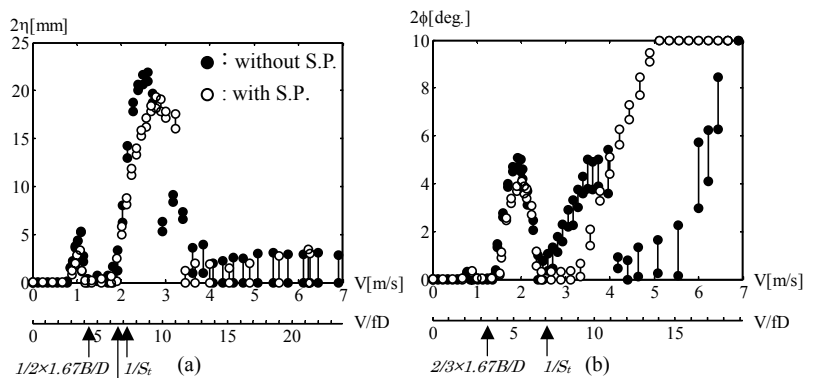


Fig. 2 V-A diagram of (a) Heaving 1DOF and (b) Torsional 1DOF

**Keywords** Proper orthogonal decomposition, Unsteady pressure, Rectangular section

連絡先 〒606-8501 京都市左京区吉田本町 京都大学大学院工学研究科社会基盤工学専攻 TEL 075-753-5093

### 3. ANALYSIS OF RESULTS

In this research, a series of free vibration tests and unsteady pressure tests for oscillating rectangular cylinder with the side ratio 4 were carried out. The eigenvalue  $\lambda$  and the eigenvectors  $\Phi$  of the covariance matrix  $R_p$  of the unsteady pressure distribution were calculated for the fixed model and for the oscillating model at various response regimes confirmed by free vibration tests. For almost all cases the first two modes provide 90% of total energy of the pressure fluctuations. It is confirmed that there is about  $90^\circ$  phase-lag between 1<sup>st</sup> and 2<sup>nd</sup> principal components. In order to investigate the physical meaning of proper functions, they were compared with the variation of instantaneous pressure distribution around the body during a 1cycle body oscillation. As a result, it is observed that 1<sup>st</sup> & 2<sup>nd</sup> proper functions are approximately identical with the pressure distribution at particular timings of the body oscillation. Besides it is also confirmed that there is  $90^\circ$  phase-lag between the particular timings. The  $\theta$  is calculated between the particular timing and maximum relative angle of attack which is defined as  $0^\circ$ . As shown fig. 7, the 1<sup>st</sup> & 2<sup>nd</sup> proper functions are identical with the pressure distribution at (a) and (b), and the reversed shape of 1<sup>st</sup> & 2<sup>nd</sup> proper functions are observed at (a)\* and (b)\* which have  $180^\circ$  phase with respect to the (a) and (b) respectively. Between reduced velocity 8 and 12 the 1<sup>st</sup> proper function is changed considerably from that at low-reduced velocity; the first zero cross point moves to the mid-chord from the leading-edge part and second zero cross point is over. It seems that these variations are induced by the velocity-increase of vortex convection on the side surface of the body as increase of reduced wind velocity.

### 4. CONCLUSION & FUTURE WORK

In POD analysis, it is inevitable to investigate the physical meaning of proper function in order to interpret the mechanisms of aerodynamic phenomena. As a result, it seems that proper functions represent instantaneous pressure distribution around the body. It is necessary to research the physical factors which determine the dominant proper functions and their contribution ratio in POD analysis.

### REFERENCE

M.Matsumoto et.al.: Vortex-induced vibrations and the vortex interferences to aerodynamic instabilities on the rectangular section with side ratio 4, *The 17th KCCNN Symposium on Civil Engineering.*, pp.261-266, 2004.

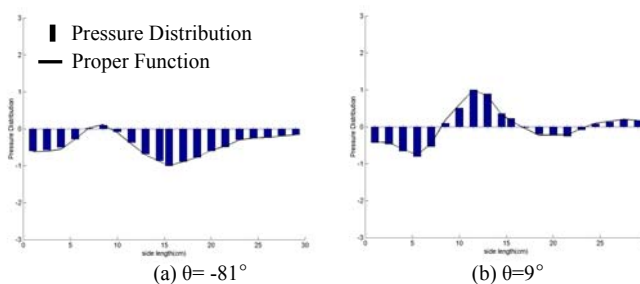


Fig. 3 Heaving motion with S.P. [V/fD=4.53] 1<sup>st</sup> & 2<sup>nd</sup> proper functions

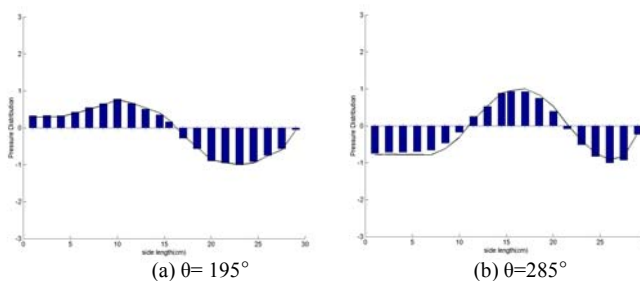


Fig. 4 Heaving motion with S.P. [V/fD=10.67] 1<sup>st</sup> & 2<sup>nd</sup> proper functions

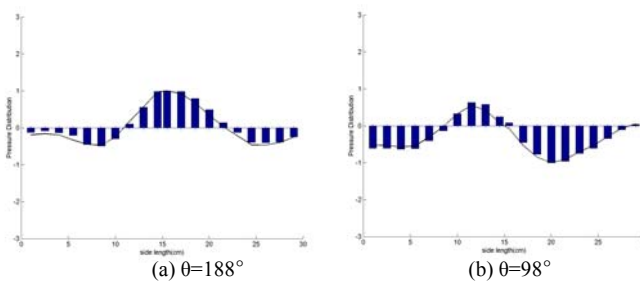


Fig. 5 Torsional motion with S.P. [V/fD=5.33] 1<sup>st</sup> & 2<sup>nd</sup> proper functions

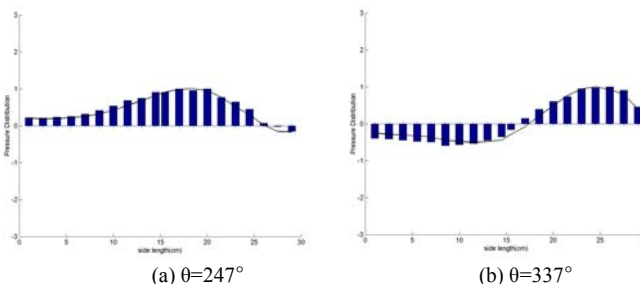


Fig. 6 Torsional motion with S.P. [V/fD=13.33] 1<sup>st</sup> & 2<sup>nd</sup> proper functions

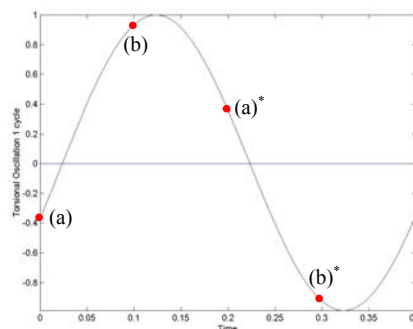


Fig. 7 Torsional oscillation with S.P. [V/fD=13.33]